Human Genetics (2019) 138:1391–1407
https://doi.org/10.1007/s00439-019-02084-8

ORIGINAL INVESTIGATION

High-throughput transcriptome analysis reveals that the loss of *Pten* activates a novel NKX6-1/RASGRP1 regulatory module to rescue microphthalmia caused by *Fgfr2*-deficient lenses

Stephanie L. Padula[1] · Deepti Anand[2] · Thanh V. Hoang[1,4] · Blake R. Chaffee[1] · Lin Liu[1] · Chun Liang[1] · Salil A. Lachke[2,3] · Michael L. Robinson[1]

Received: 16 August 2019 / Accepted: 28 October 2019 / Published online: 5 November 2019
© Springer-Verlag GmbH Germany, part of Springer Nature 2019

Abstract

FGFR signaling is critical to development and disease pathogenesis, initiating phosphorylation-driven signaling cascades, notably the RAS-RAF-MEK-ERK and PI3 K-AKT cascades. PTEN antagonizes FGFR signaling by reducing AKT and ERK activation. Mouse lenses lacking FGFR2 exhibit microphakia and reduced ERK and AKT phosphorylation, widespread apoptosis, and defective lens fiber cell differentiation. In contrast, simultaneous deletion of both *Fgfr2* and *Pten* restores ERK and AKT activation levels as well as lens size, cell survival and aspects of fiber cell differentiation; however, the molecular basis of this "rescue" remains undefined. We performed transcriptomic analysis by RNA sequencing of mouse lenses with conditional deletion of *Fgfr2*, *Pten* or both *Fgfr2* and *Pten*, which reveal new molecular mechanisms that uncover how FGFR2 and PTEN signaling interact during development. The FGFR2-deficient lens transcriptome demonstrates overall loss of fiber cell identity with deregulated expression of 1448 genes. We find that ~ 60% of deregulated genes return to normal expression levels in lenses lacking both *Fgfr2* and *Pten*. Further, application of customized filtering parameters to these RNA-seq data sets identified 68 high-priority candidate genes. Bioinformatics analyses showed that the *cis*-binding motif of a high-priority homeodomain transcription factor, NKX6-1, was present in the putative promoters of ~ 78% of these candidates. Finally, biochemical reporter assays demonstrate that NKX6-1 activated the expression of the high-priority candidate *Rasgrp1*, a RAS-activating protein. Together, these data define a novel regulatory module in which NKX6-1 directly activates *Rasgrp1* expression to restore the balance of ERK and AKT activation, thus providing new insights into alternate regulation of FGFR downstream events.

Introduction

Fibroblast growth factor receptor (FGFR) signaling plays a critical role in the development of nearly every mammalian tissue, and FGFR mutations cause numerous human conditions including several craniosynostosis syndromes (Crouzon syndrome, Pfeiffer syndrome, Craniosynostosis, Apert syndrome, Jackson–Weiss syndrome, Beare–Stevenson cutis gyrata syndrome, and Saethre–Chotzen syndrome) as well as the most common forms of human dwarfism (achondroplasia, hypochondroplasia and thanatophoric dysplasia) (Reviewed in Marie et al. 2005; Sawh-Martinez and Steinbacher 2019). In addition, overexpression or aberrant signaling of FGFRs contributes to many different human cancers including gastric, urothelial, endometrial, breast, prostate, lung, liver, brain, head and neck, ovarian and thyroid carcinomas (Reviewed in Babina and Turner 2017).

Electronic supplementary material The online version of this article (https://doi.org/10.1007/s00439-019-02084-8) contains supplementary material, which is available to authorized users.

✉ Michael L. Robinson
robinsm5@miamioh.edu

[1] Department of Biology, Miami University, Oxford, OH 45056, USA

[2] Department of Biological Sciences, University of Delaware, Newark, DE, USA

[3] Center for Bioinformatics and Computational Biology, University of Delaware, Newark, DE, USA

[4] Present Address: Department of Neuroscience, Johns Hopkins School of Medicine, Baltimore, MD, USA

FGFR signaling also performs essential functions in development, survival and differentiation of the ocular lens (McAvoy and Chamberlain 1989; Robinson et al. 1995; Lovicu and Overbeek 1998; Madakashira et al. 2012; Li et al. 2014, 2019; Zhao et al. 2008; Chow et al. 1995; Garcia et al. 2005, 2011; Collins et al. 2018). Isolated deletion of *Fgfr2* (one of three *Fgfrs* expressed in the developing lens) at the lens placode stage results in microphakia (small lenses) due to defective fiber cell differentiation and widespread apoptosis in the lens without significant alterations of cell proliferation (Garcia et al. 2005, 2011; Chaffee et al. 2016). Given the dependence of eye size on lens size, microphakia inevitably leads to microphthalmia. FGFR2-deficient lenses also exhibit significantly lowered levels of activated intracellular kinases ERK and AKT (Chaffee et al. 2016), which are responsible for many of the downstream effects of FGFR signaling. Approximately 25% of patients with microphthalmia have been linked to causative gene mutations including the transcription factors PAX6, OTX2, SOX2, and VSX2 (Verma and Fitzpatrick 2007), but no direct link between FGFR signaling and microphthalmia has been established in humans. Interestingly, the majority of microphthalmia cases appear in conjunction with non-ocular developmental deformities that include craniofacial abnormalities. Despite this, the relationship between aberrant FGFR signaling, craniosynostosis, and microphthalmia remains poorly understood in humans.

The ocular lens consists of only two co-existing cell types, epithelial cells and fiber cells, encased in a thick lens capsule to form an isolated system within the eye. These two cell types form a relatively simple pattern of epithelial cell proliferation and terminal fiber cell differentiation throughout the vertebrate lifespan. This feature of continuous, spatially restricted proliferation and differentiation makes the lens an excellent model to investigate the regulation and role of FGFR signaling in cell survival, growth, and differentiation (Wormstone et al. 2011; Cvekl and Zhang 2017). Despite abundant evidence that FGFR signaling provides essential support for cell survival and differentiation in the lens and in other extra-ocular tissues, the molecular mechanism by which FGFR activation leads to altered gene expression during vertebrate development remains incomplete.

The tumor-suppressor PTEN (phosphatase and tensin homolog) is a dual-specificity phosphatase that negatively regulates FGFR signaling, in part by inhibiting the activation of AKT (Myers et al. 1997) and in part by inhibiting the activation of RAS, a protein upstream of ERK1/2 activation. FGFR signaling activates PI3 kinase (PI3 K) which phosphorylates phosphatidylinositol (4,5)-bisphosphate (PIP2) to create phosphatidylinositol (3,4,5)-triphosphate (PIP3), an essential activator of AKT. In contrast, PTEN dephosphorylates PIP3 to PIP2, thereby preventing PIP3-mediated AKT activation (Stambolic et al. 1998). PTEN also dephosphorylates the adapter protein SHC, therefore inhibiting another FGFR downstream signaling event, namely the recruitment of the GRB2/SOS complex and the activation of RAS along the RAS-RAF-MEK-ERK pathway (Gu et al. 1998; Kanai et al. 1997; Klint et al. 1999; Mohammadi et al. 1996). In addition to its role in regulating FGFR signaling, PTEN abnormalities cause numerous human diseases including PTEN hamartoma tumor syndrome that includes multiple subtypes: Cowden syndrome, Bannayan–Riley–Ruvalcaba syndrome, and Proteus-like syndrome (Liaw et al. 1997; reviewed in Pilarski 2019), autism (Butler et al. 2005), and cancers of the breast, endometrium, thyroid, brain, prostate, lung, skin, adrenal glands and hematopoietic system (Reviewed in Hollander et al. 2011). Isolated deletion of *Pten* in the developing mouse lens results in progressive age-related cataracts due to increased intracellular hydrostatic pressure and sodium concentrations, but PTEN-deficient lenses exhibit relatively normal prenatal morphological development (Sellitto et al. 2013; Chaffee et al. 2016). Of note, PTEN stabilization by thalidomide contributes to microphthalmia observed in human and chick embryos exposed to this teratogen (Knobloch et al. 2008).

Several studies highlight the importance of PTEN for the regulation of FGFR signaling in various cell types such as osteoprogenitor cells, adipocytes, and keratinocytes (Guntur et al. 2011; Scioli et al. 2014; Hertzler-Schaefer et al. 2014). Likewise, in the developing lens, simultaneous *Pten* deletion rescues the apoptosis and some defects in fiber cell differentiation observed upon *Fgfr2* deletion (Chaffee et al. 2016). The deletion of *Pten* raised the level of both AKT and ERK1/2 phosphorylation in *Fgfr2*-deficient lenses. These *Fgfr2/Pten*$^{\Delta/\Delta}$ lenses also normalized the levels of phosphorylation of p53 (Ser15), c-JUN and MDM2, away from the proapoptotic state (high phosphorylation of c-JUN and p53 and low phosphorylation of MDM2) seen in *Fgfr2*$^{\Delta/\Delta}$ lenses. Further, *Pten* deletion partially rescued fiber cell elongation and the expression of *γ-crystallins*. The restoration of some aspects of lens development in lenses lacking *Fgfr2* by the simultaneous deletion of *Pten* provides a unique opportunity to mechanistically dissect how FGFR signaling directs tissue development.

To better understand how PTEN regulates FGFR2-signaling during eye development, we undertook an RNA-seq analysis followed by functional validation. This global transcriptional analysis revealed that *Fgfr2* deletion in the lens causes widespread deregulation of genes related to p53-mediated apoptosis, cell migration, and the lens structure. However, simultaneous deletion of *Pten* (*Fgfr2/Pten*)$^{\Delta/\Delta}$ results in the "rescue" of ~ 60% of genes deregulated in *Fgfr2*$^{\Delta/\Delta}$ lenses to control levels, thus offering insights into the molecular basis of the rescue of the phenotypic defects in these animals. Bioinformatic analysis of transcripts deregulated in the *Fgfr2*$^{\Delta/\Delta}$ lenses but restored

in the $(Fgfr2/Pten)^{\Delta/\Delta}$ lenses led to the identification of high-priority genes that may function in the rescue phenotype as novel regulators of FGFR signaling. From this, we identified the homeodomain transcription factor *Nkx6-1*, as a potential new regulator of FGFR downstream targets in the lens. We show that NKX6-1 activates the downstream target *Rasgrp1*, a guanine nucleotide exchange factor and PI3 K-AKT and MAPK activator, defining a new regulatory relationship between this transcription factor and signaling pathways. This pathway provides a molecular explanation for the mechanism contributing to PTEN-mediated rescue of FGFR signaling. Given the general biological importance of both FGFR signaling and PTEN in human development and disease, these novel revelations extend the molecular understanding of disorders characterized by aberrant FGFR signaling or mutations in *Pten* (Liaw et al. 1997; Butler et al. 2005; McIntosh et al. 2000).

Materials and methods

Animals

Newborn *FVB/N*, *Le-Cre*, and *Le-Cre* mice with two loxP flanked (floxed) alleles of *Fgfr2*, *Pten*, or *Fgfr2* and *Pten* were euthanized with CO_2 inhalation before the lenses were removed. All mice were maintained on an *FVB/N* genetic background. All procedures were approved by the Miami University Institutional Animal Care and Use Committee and complied with the ARVO Statement for the Use of Animals in Research and consistent with those published by the Institute for Laboratory Animal Research (Guide for the Care and Use of Laboratory Animals).

RNA sequencing (RNA-Seq) library preparation and sequencing

We collected RNA from the lenses of mice hemizygous for the *Le-Cre* transgene (control), or hemizygous for *Le-Cre* and homozygous for loxP flanked (floxed) alleles of *Fgfr2* ($Fgfr2^{\Delta/\Delta}$), *Pten* ($Pten^{\Delta/\Delta}$); or both ($(Fgfr2/Pten)^{\Delta/\Delta}$). Hemizygous *Le-Cre* mice were used as controls given the moderate changes in gene expression between hemizygous *Le-Cre* and *FVB/*N lenses (Lam et al. 2019). Lenses were dissected from the eye and carefully isolated from surrounding tissues including the cornea, retina, and tunica vasculosa lentis. Lenses were pooled into three biological replicates for each genotype, with each replicate containing six lenses from three mice. Total RNA was isolated from each replicate using the mirVana isolation kit (Ambion, Life Technologies, Grand Island, NY). Total RNA samples with the RNA integrity number (RIN, Agilent 2100 Bioanalyzer) ≥ 8.0 were used to prepare a library of template molecules suitable for subsequent sequencing on an Illumina (St. Louis, MO) HiSeq platform. Polyadenylated RNA was purified from the total RNA samples using Oligo dT conjugated magnetic beads and prepared for single-end sequencing according to the Illumina TruSeq RNA Sample Preparation Kit v3. All the libraries were sequenced using the TruSeq SBS kit on an Illumina HiSeq 2000 at the Genomics and Sequencing Core Laboratory at the University of Cincinnati. The raw and processes data files are deposited to NCBI GEO (accession number GSE132945).

RNA-seq data pre-processing and quality analysis

The obtained raw RNA-seq data sets were evaluated for sequence quality (per-base sequence quality, sequence length distribution, overrepresented adapter/primer sequences) using the FastQC tool available at http://www.bioinformatics.babraham.ac.uk/projects/fastqc/. Sequence trimming of leading and trailing low-quality reads (phred < 28), ambiguous bases (N), sequencing adapters, primers was performed with Trimmomatic tool (Bolger et al. 2014). The trimmed reads were mapped to the *Mus musculus* reference genome (GRCm38/mm10) using Tophat v2.0.9 (Trapnell et al. 2009). The obtained BAM files from all the data sets were used to compute transcript-level expression through Cufflinks (Trapnell et al. 2012). The expression data in counts per million (CPM) was imported in EdgeR package (Robinson et al. 2010) available at https://bioconductor.org and data normalization was performed using the Trimmed Mean of M-values (TMM) method. Differential gene expression between comparisons $Fgfr2^{\Delta/\Delta}$ vs. *Le-Cre*, $Pten^{\Delta/\Delta}$ vs. *Le-Cre* and $Fgfr2/Pten^{\Delta/\Delta}$ vs. *Le-Cre* was computed as $\log_2$ fold-change (FC) using the "quasi-likelihood" (QF-) test included in EdgeR package. Genes with cutoff values of ≥ 0.5 $\log_2$ FC at $p < 0.05$, and expression in counts per million (CPM) cutoff ≥ 1.0 in at least one sample were consider for the downstream bioinformatics analysis as previously described (Cavalheiro et al. 2017). To evaluate global RNA-seq gene expression profiles, principle component analysis (PCA) was performed using R-function to obtain a 3D visualization for $Fgfr2^{\Delta/\Delta}$, $Pten^{\Delta/\Delta}$, $Fgfr2/Pten^{\Delta/\Delta}$, and *Le-Cre* individual replicates.

Integrated downstream bioinformatics analysis of differentially expressed genes

We performed gene ontology (GO) functional annotation analysis on the differentially expressed genes (DEGs) from the comparisons between different genotypes (e.g. $Fgfr2^{\Delta/\Delta}$ vs. *Le-Cre*; $Fgfr2/Pten^{\Delta/\Delta}$ vs. *Le-Cre*). The DEG criterion included those genes for which in the knockout genotypes (e.g. $Fgfr2^{\Delta/\Delta}$; $Fgfr2/Pten^{\Delta/\Delta}$), there was a ≥ 0.5 $\log_2$ FC at $p < 0.05$, and expression CPM cutoff of ≥ 1.0 compared to

Le-Cre. DEGs were identified and GO functional annotation was performed using Database for Annotation, Visualization and Integrated Discovery (DAVID) bioinformatics resource (Huang et al. 2009). These data were then analyzed in the context of normal lens expression data sets using iSyTE. Normal embryonic and postnatal lens expression data for DEGs identified from comparisons *Fgfr2*$^{\Delta/\Delta}$ vs. *Le-Cre*, *Pten*$^{\Delta/\Delta}$ vs. *Le-Cre* and *Fgfr2/Pten*$^{\Delta/\Delta}$ vs. *Le-Cre* were obtained from iSyTE 2.0 lens gene database (Kakrana et al. 2018). The significance for the iSyTE 2.0 lens enriched expression was estimated using Chi square (χ^2) test for goodness of fit followed by a two-tailed *t* test. The data were presented in a quadrant plot using an in-house *Python* script. This was followed by derivation of an integrative network for candidate genes associated with *Pten*-mediated rescue of *Fgfr2* deficient lens. We used the following two filters to identify DEGs that correlate with the "rescue" of the lens defects by simultaneous deletion of *Pten* in the *Fgfr2/Pten*$^{\Delta/\Delta}$. Filter 1: Genes that satisfy the following three criteria: (a) are downregulated in lenses of *Fgfr2*$^{\Delta/\Delta}$ compared to *Le-Cre*, (b) are upregulated in *Pten*$^{\Delta/\Delta}$ compared to *Le-Cre*, and (c) are upregulated or exhibit no-change in *Fgfr2/Pten*$^{\Delta/\Delta}$ compared to *Pten*$^{\Delta/\Delta}$. Filter 2: Genes that satisfy the following three criteria (a) are downregulated in lenses of *Fgfr2*$^{\Delta/\Delta}$ compared to *Le-Cre*, (b) are upregulated in *Pten*$^{\Delta/\Delta}$ compared to *Le-Cre*, and (c) are upregulated or exhibit no-change in *Fgfr2/Pten*$^{\Delta/\Delta}$ compared to *Fgfr2*$^{\Delta/\Delta}$. Filter 1 and 2 identified 28 and 40 genes, respectively. An integrative approach was taken to derive a gene regulatory network for these 68 genes. Protein–protein interaction (PPI) data were extracted from the String database (http://string-db.org), and *cis*-regulatory DNA-binding motifs were obtained for the transcription factors GATA6, EVX2, and NKX6-1 from motif database MotifDb (http://bioconductor.org). The motifs for GATA6, EVX2, and NKX6-1 were searched in the 2500 bp region upstream of the transcription start site (TSS) of the 68 genes. An in-house Python script was used to read data from PPI, *cis*-regulatory motif analysis and lens gene expression from iSyTE. The integrative network was visualized in Cytoscape (www.cytoscape.org).

Validation of candidate genes identified from integrated bioinformatics approach

To validate the candidate genes identified from the RNA-Seq data, the expression level of selected genes was analyzed with RT-qPCR. Genes were chosen based on integrated bioinformatics approach using (1) high expression and/or enrichment in the lens based on iSyTE database, (2) or based on biological significance obtained from GO analysis. The RNA samples used for RNA-Seq were reverse-transcribed into cDNA, using random primers and Superscript IV reverse transcriptase (Invitrogen), according to the manufacturer's instructions. The RT-qPCR assays were performed in triplicate on the cDNA using GoTaq Green Master Mix (Promega, Madison, WI) following the manufacturer's instructions and read using a CFX connect instrument (Bio-Rad, Hercules, CA). Intron-spanning primers were designed to specifically quantify targeted mRNA transcripts (Online Resource 6). Glyceraldehyde 3-phosphate dehydrogenase (GAPDH) expression was used as an internal control. The cycling conditions consisted of 1 cycle at 95 °C for 100 s for denaturation, followed by 40 three-step cycles for amplification (each cycle consisted of 95 °C incubation for 20 s, an appropriate annealing temperature for 10 s, and product elongation at 70 °C incubation for 20 s). The presence of the melting curve and a single DNA band on agarose gels following RT-qPCR amplification was monitored to determine reaction specificity. The quantification cycle (*C*q) was obtained from the RT-qPCR, and the ΔCq value was calculated as $C\text{q}_{\text{(gene)}} - C\text{q}_{\text{(GAPDH)}}$. The data are expressed as mean ± the standard error of the mean.

Luciferase assay

To determine whether NKX6-1 drives the expression of *Rasgp1* and *Fgfr2* in lens epithelial cells, murine 21EM15 cells (Reddan et al. 1989) were grown in DMEM supplemented with 10% fetal bovine serum, 1% non-essential amino acids, and 1% anti–anti until confluency at which point they were passaged twice. After reaching 80% confluence, the cells were transfected using Turbofect Transfection Reagent (ThermoFisher #R0531) with the appropriate vectors following the manufacturer's protocol. The vectors used for cloning and transfection were pGL4.10[*luc2*] (New England Biolabs #E6651) pRL-TK (Promega #E2231), and Tet-O-FUW-Nkx6-1 (Addgene #45846). The putative promoter regions of mouse *Rasgrp1* and *IL-6* (2500 bp region upstream of the transcription start site for each gene), were cloned into the pGL4.10[*luc2*] vector separately using the Gibson Assembly Cloning Kit from New England Biolabs (NEB). A mouse lens epithelial cell line (21EM15) was transfected with pGL4.10[luc2] and, after transfection, cells were seeded on a 96-well plate for 36 h prior to collection and lysis. Luciferase assays were carried out using the Dual-Luciferase Reporter Assay System (Promega E1910) according to the manufacturer's instructions, and analyzed on the Synergy H1 microplate reader (BioTek, VT).

Results

FGFR2 signaling regulation by PTEN in both the periocular skin and in the lens

To provide a brief overview, we confirmed the gross external and histological phenotypes of *Le-Cre*-mediated deletion of *Fgfr2* and/or *Pten* in mice (Fig. 1). In agreement with earlier findings (Hertzler-Schaefer et al. 2014), the deletion of *Pten* alone in the ocular surface ectoderm leads to the formation of multiple, postnatal skin tumors corresponding to the pattern of CRE-mediated deletion in *Le-Cre* mice, and these tumors do not form in the absence of both *Pten* and *Fgfr2* (Fig. 1a). Lenses lacking FGFR2 appear small and exhibit several abnormalities at birth, including microphakia (Fig. 1b). In contrast, newborn lenses lacking both FGFR2 and PTEN demonstrate a nearly complete rescue of lens size despite still having aspects of abnormal development. Lenses hemizygous for the *Le-Cre* transgene or lacking only PTEN display normal size and morphology at birth. The simultaneous loss of both *Pten* and *Fgfr2* fails to rescue the inability of *Fgfr2*-deficient eyes to complete eyelid closure. The histological

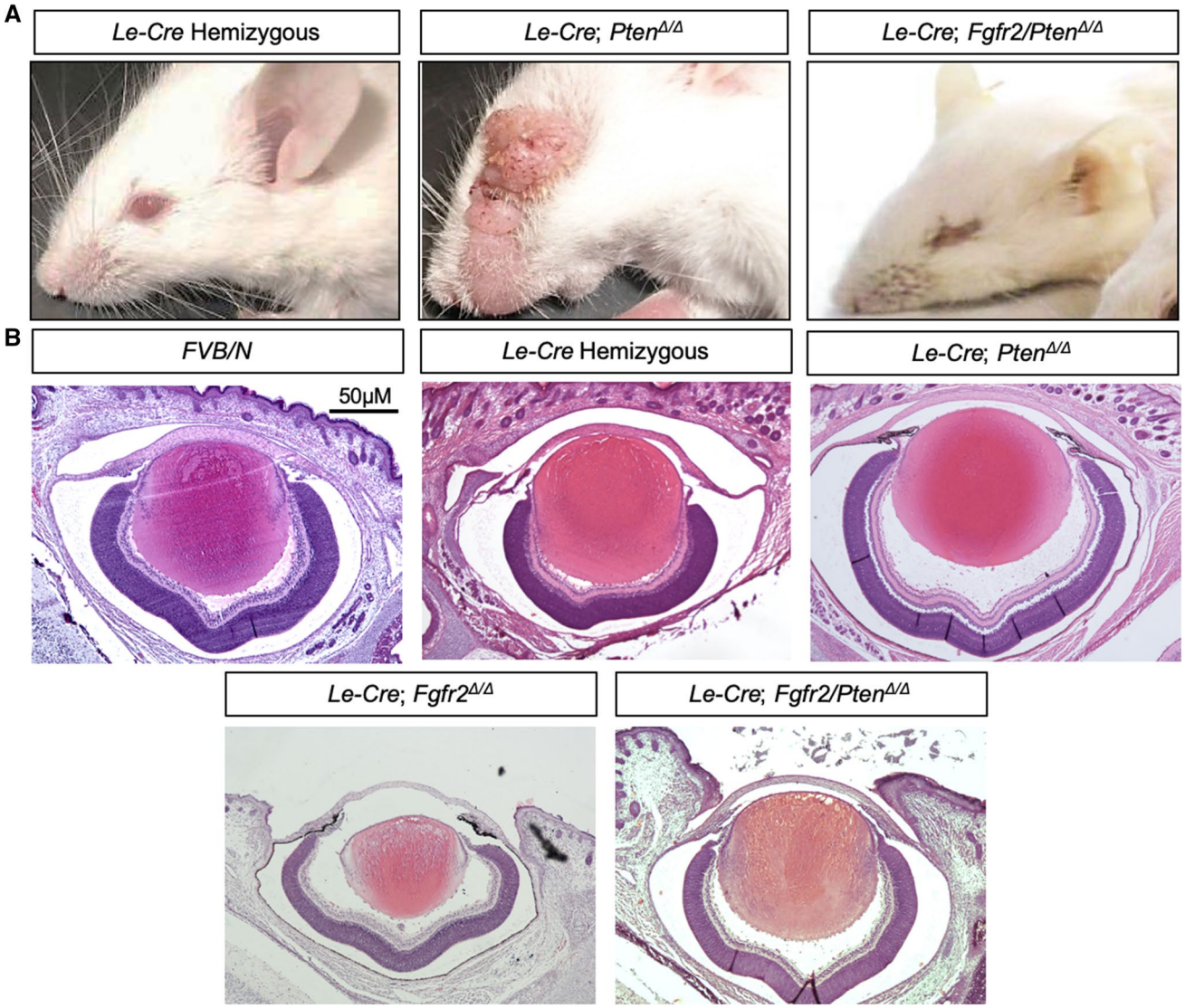

Fig. 1 **a** Within a month after birth, the skin surrounding the eye and extending to the nose develop rapidly growing tumors in the absence of *Pten* alone (*Le-Cre*; *Pten*$^{\Delta/\Delta}$). However, these tumors fail to form in skin lacking both *Pten* and *Fgfr2* (*Le-Cre*; *Fgfr2/Pten*$^{\Delta/\Delta}$). Mice in which *Le-Cre* mediates the deletion of *Fgfr2* alone (*Le-Cre; Fgfr2*$^{\Delta/\Delta}$) do not look externally different than *Le-Cre*; *Fgfr2/Pten*$^{\Delta/\Delta}$ mice (not shown). Mice hemizygous for the *Cre* transgene alone (*Le-Cre Hemizygous*) exhibit normal external appearance. **b** Postnatal day 0 (P0) lens sections for controls (*FVB/N* and *Le-Cre Hemizygous)*, *Pten*-deficient (*Le-Cre*; *Pten*$^{\Delta/\Delta}$), *Fgfr2*-deficient (*Le-Cre*; *Fgfr2*$^{\Delta/\Delta}$), and lenses lacking both *Fgfr2* and *Pten* (*Le-Cre*; *Fgfr2/Pten*$^{\Delta/\Delta}$)

phenotypes of lenses lacking *Fgfr2, Pten* or both *Fgfr2* and *Pten* were previously described in detail in Chaffee et al. (2016).

To understand the transcriptional programs directed by FGFR signaling during development and their relevance to the ocular defect microphakia, we conducted an RNA-Seq analysis on newborn mouse lenses lacking individually *Fgfr2* or *Pten*, or both *Fgfr2* and *Pten*. By conducting this analysis, we sought to (1) define the transcriptional events directed by FGFR2 signaling that are perturbed in the $Fgfr2^{\Delta/\Delta}$ lenses, (2) determine the major genes and associated pathways that are involved in $Pten^{\Delta/\Delta}$-mediated rescue of the defects in the FGFR2 deficient lens, and (3) identify novel regulators of development downstream of FGFR signaling and PTEN activity. Specifically, we focused on genes and gene networks relevant to cell survival, fiber cell differentiation, and AKT and ERK1/2 downstream modules, the processes most profoundly affected by *Fgfr2* loss. Figure 2 provides a schematic diagram of our approach.

Overview of *Le-Cre*, $Fgfr2^{\Delta/\Delta}$, $Pten^{\Delta/\Delta}$, and *Fgfr2*/$Pten^{\Delta/\Delta}$ lens transcriptomes

RNA-seq provided a non-biased mechanism to collect transcript profiles from newborn mouse lenses lacking *Fgfr2* ($Fgfr2^{\Delta/\Delta}$), *Pten* ($Pten^{\Delta/\Delta}$), both *Fgfr2* and *Pten* (*Fgfr2*/$Pten^{\Delta/\Delta}$) and hemizygous *Le-Cre* (the transgenic allele that mediates conditional gene deletion) control lenses. Each biological sample contained six lenses from a total of three mice, with three replicates for a total of nine mice per genotype. Each biological replicate generated between 25.5 and 34.5 million 50 bp sequence reads. On average, 93.4% of $Fgfr2^{\Delta/\Delta}$ reads, 91.6% of $Pten^{\Delta/\Delta}$ reads, 94.0% of *Fgfr2*/$Pten^{\Delta/\Delta}$ reads, and 91.5% of *Le-Cre* reads mapped to the reference *Mus musculus* genome (GRCm38/mm10) (Table 1).

Principle component analysis of all gene expression datasets identified trends in the data set by reducing the dimensionality of the data. The resulting plot revealed that biological replicates from each sample group clustered reasonably close together, indicating a high overall similarity within replicates of the same genotype (Fig. 3a). The variable along principle components 1 and 2 separates the $Fgfr2^{\Delta/\Delta}$ replicates dramatically from the other three genotypes. Likewise, principle component 3 distinguishes the *Le-Cre* replicates from the $Fgfr2^{\Delta/\Delta}$, $Pten^{\Delta/\Delta}$ and *Fgfr2*/$Pten^{\Delta/\Delta}$ replicates. $Pten^{\Delta/\Delta}$ and *Fgfr2*/$Pten^{\Delta/\Delta}$ replicates group closely together along all three principle components.

Deletion of *Fgfr2*, *Pten* or both *Pten* and *Fgfr2* caused massive deregulation of gene expression relative to *Le-Cre* lenses (Fig. 3b). Isolated deletion of *Fgfr2* resulted in the downregulation of 661 genes and the upregulation of 787 genes (Online Resource 1). Deletion of *Pten* alone caused a decrease in the expression of 485 genes and an increase in the expression of 489 genes in the lens (Online Resource 2). *Fgfr2*/$Pten^{\Delta/\Delta}$ lenses exhibited 674 downregulated and 446 upregulated genes, respectively (Online Resource 3). The list of top DEGs (excluding the pseudogenes) from all three comparisons $Fgfr2^{\Delta/\Delta}$ vs. *Le-Cre*, $Pten^{\Delta/\Delta}$ vs. *Le-Cre* and *Fgfr2*/$Pten^{\Delta/\Delta}$ vs. *Le-Cre* are presented in Tables 2, 3, and 4, respectively.

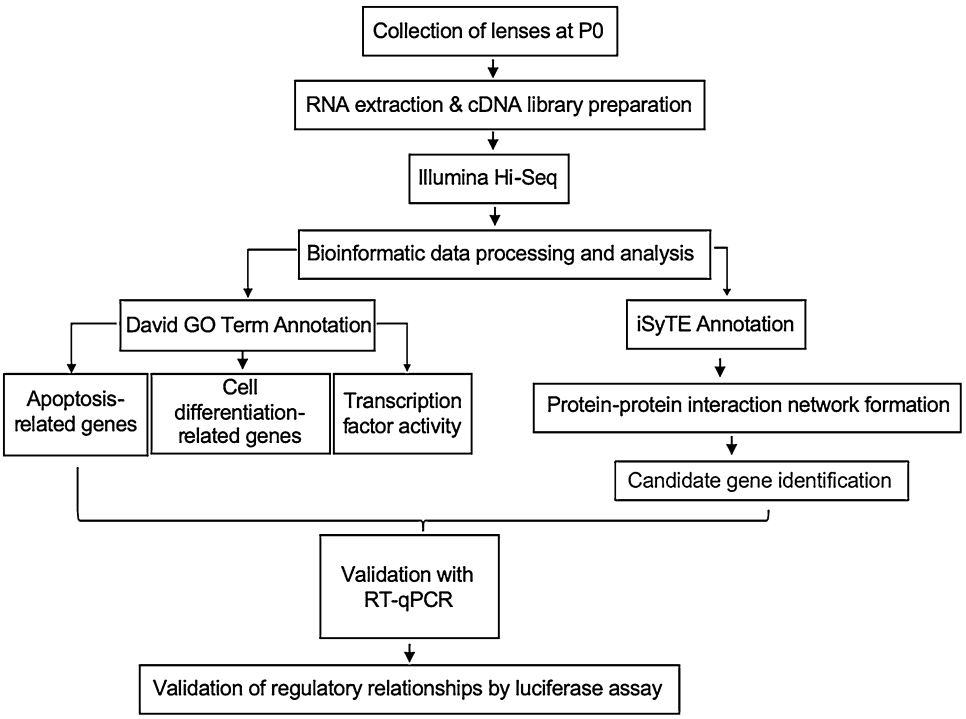

Fig. 2 Graphical abstract and workflow of the study

Table 1 Overview of read alignments for RNA-seq

Sample name	Abbreviation	Total number of reads	Reads mapped to the genome	Alignment percentage (%)
Le-Cre	L1	34450874	31117864	90.30
	L2	29745513	27775531	93.50
	L3	27806619	25195812	90.60
$Fgfr2^{\Delta/\Delta}$	R1	27850644	26083275	93.70
	R2	24810082	23061821	93.00
	R3	28871246	27020465	93.60
$Pten^{\Delta/\Delta}$	P1	31200642	28032031	89.80
	P2	28622748	26009802	90.90
	P3	25530167	24029149	94.10
$Fgfr2/Pten^{\Delta/\Delta}$	PR1	26252406	24787739	94.40
	PR2	26243385	24728575	94.20
	PR3	29629966	29529966	93.50

For each genotype (sample name), three biological replicates (abbreviation) containing six lenses each were pooled, extracted of RNA, and sequenced. These reads were then mapped to the *Mus musculus* genome. The alignment percentage is percentage of total reads mapped to the reference genome

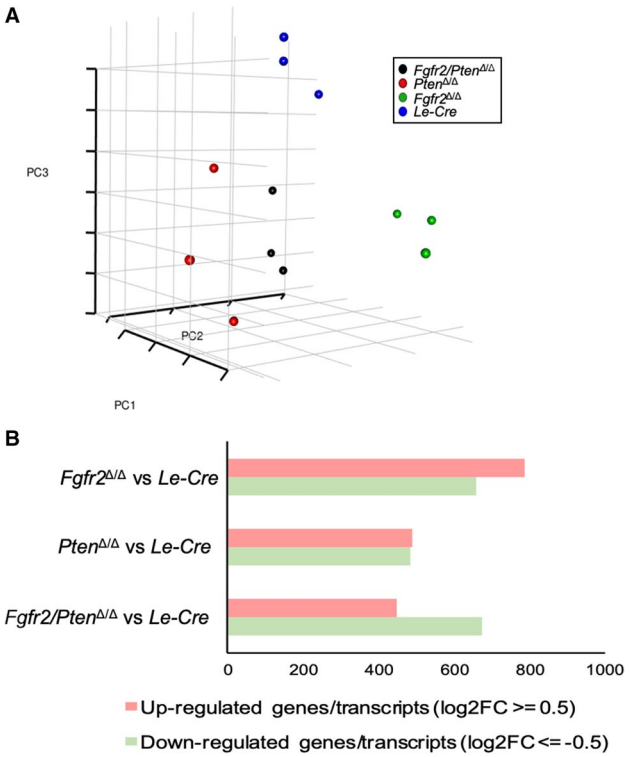

Fig. 3 **a** Principle component analysis of genes deregulated in *Le-Cre* (blue), $Pten^{\Delta/\Delta}$ (red), $Fgfr2^{\Delta/\Delta}$ (green), and $Fgfr2/Pten^{\Delta/\Delta}$ (black) lenses. **b** Total number of upregulated genes/transcripts (red) and downregulated genes/transcripts (green) in each genotype relative to *Le-Cre*

Table 2 Top differentially expressed genes (DEGs) in *Fgfr2*-deleted lenses

Downregulated		Upregulated	
Gene symbol	Log2 FC	Gene symbol	Log2 FC
Spta1	−5.8	*Cryga*	22.2
Clic5	−4.0	*Cryge*	19.7
Aqp3	−3.9	*Dynlt1b*	9.2
Tuba1c	−3.5	*Rps3a3*	8.7
Fmn2	−3.2	*Csmd1*	8.1
Cd44	−3.1	*Col1a1*	5.7
Evx2	−3.1	*Cwc22*	4.9
Fbxo44	−3.0	*Rtn1*	4.1
Rasgrp1	−3.0	*Papss2*	4.0
Wdr43	−2.8	*Pkd1l1*	3.8
Sv2c	−2.3	*Aph1b*	3.5
Actr2	−2.3	*Gstp2*	3.5
Gata6	−2.2	*Abca13*	3.4
Cntn4	−2.2	*Jakmip3*	3.3
Tbc1d30	−2.2	*Far2os1*	3.3
Gjb6	−2.2	*Cox6a2*	3.2
Atg3	−2.2	*Fcnb*	3.1
Cxcl12	−2.1	*Col3a1*	3.0
Frzb	−2.0	*Htr1d*	3.0
Csmd2	−1.9	*Stk32c*	2.5

The official gene symbol along with the log2 fold-change value for the 20 most downregulated and 20 most upregulated genes in *Fgfr2*-deleted lenses compared to control (*Le-Cre)* lenses are listed

In any comprehensive transcriptome analysis, distilling massive amounts of data into biologically relevant insights represents a major challenge. In our data set, the genes deregulated solely by *Pten* represent an interesting story. However, the regulation of FGFR signaling by PTEN during lens development—specifically, the molecular pathways

Table 3 Top differentially expressed genes (DEGs) in *Pten*-deleted lenses

Downregulated		Upregulated	
Gene symbol	Log2 FC	Gene symbol	Log2 FC
Actr2	−8.4	*Dynlt1b*	9.2
Wdr43	−5.2	*Gm15772*	8.7
Sgip1	−3.1	*Cwc22*	4.8
Penk	−2.3	*Chac1*	4.3
Pbld2	−2.1	*Pkd1l1*	3.8
Zfp626	−1.9	*Csmd1*	3.7
Sv2c	−1.9	*Gm24265*	3.6
Egfem1	−1.7	*Jakmip3*	3.3
Dock9	−1.7	*Slc1a1*	3.2
Cd247	−1.7	*Stk32c*	3.0
Tacr3	−1.7	*Acta2*	3.0
Tagap1	−1.6	*Papss2*	2.8
Cntn4	−1.6	*Eif2s3y*	2.6
Il34	−1.6	*Avp*	2.6
Stc1	−1.6	*Rsph3b*	2.5
Cnksr2	−1.6	*Tnc*	2.5
Trmt61b	−1.5	*Dkk1*	2.5
Ache	−1.5	*Tmem181a*	2.5
Abca13	−1.5	*Mylk4*	2.3
Wif1	−1.5	*Ccdc117*	2.1

The official gene symbol along with the log2 fold-change value for the 20 most downregulated and 20 most upregulated genes in *Pten*-deleted lenses compared to control (*Le-Cre)* lenses are listed

Table 4 Top differentially expressed genes (DEGs) in *Fgfr2/Pten*-deleted lenses

Downregulated		Upregulated	
Gene symbol	Log2 FC	Gene symbol	Log2 FC
Wdr43	−3.8	*Hlcs*	7.2
Spta1	−3.5	*Chac1*	4.7
Pianp	−2.9	*Cwc22*	4.2
Fgf15	−2.9	*Cox6a2*	3.8
Lrrc4c	−2.6	*Papss2*	3.4
Wif1	−2.5	*Fcnb*	3.2
Crhbp	−2.5	*Lgsn*	3.1
Tnfaip8l3	−2.4	*Stk32c*	3.0
Notumos	−2.4	*Jakmip3*	2.9
Fmn2	−2.4	*Slc1a1*	2.9
Pbld2	−2.1	*Rpgrip1*	2.8
Qtrt1	−2.0	*Eif2s3y*	2.5
Pld5	−2.0	*Sstr5*	2.5
Wfdc1	−2.0	*Acta2*	2.4
Eps8	−2.0	*Htr1d*	2.3
Vcan	−2.0	*Pkd1l1*	2.3
Cntn4	−2.0	*Ociad2*	2.2
Six6	−2.0	*Zfp809*	2.1
Actr2	−2.0	*Rdm1*	2.1
Vsx2	−1.9	*Ccdc117*	2.1

The official gene symbol along with the log2 fold-change value for the 20 most downregulated and 20 most upregulated genes in *Fgfr2/Pten*-deleted lenses compared to control (*Le-Cre)* lenses are listed

underlying the microphakia rescue—represents the focus of this manuscript. Significantly, of the 1448 genes up- or downregulated in $Fgfr2^{\Delta/\Delta}$ lenses, only 592 (40.9%) remain deregulated in the $Fgfr2/Pten^{\Delta/\Delta}$ lenses. This result demonstrates that *Pten* counterbalances FGFR2 signaling, since *Pten* deletion restores the majority of the transcripts deregulated by *Fgfr2* loss.

Analysis of apoptosis-related genes

Since apoptosis represents the major early phenotype of *Fgfr2*-deleted lenses (Chaffee et al. 2016) and contributes significantly to the microphakia phenotype, we investigated how *Fgfr2* loss affects transcripts related to cell survival by gene ontology analysis. This analysis revealed an enrichment of genes related to the regulation of apoptosis in downregulated transcripts from $Fgfr2^{\Delta/\Delta}$ lenses (Fig. 4a, Online Resource 4). Examples of these genes include *Birc7*, a caspase inhibitory protein (also known as Livin) (De Maria and Bassnett 2015), *Clu* (a chaperone protein that inhibits BAX-mediated apoptosis) (Trougakos et al. 2009), *Gadd45a* (a downstream target of p53) (Jin et al. 2003), *Pycard* (a caspase recruiting protein) (Masumoto et al. 2001), and *Pgap2* (a GPI-anchor remodeling protein) (Tashima et al. 2006). Significantly, the transcript levels of the five aforementioned genes exhibit either partial or full rescue to control (*Le-Cre*) levels by the additional deletion of *Pten*. RT-qPCR analysis validated that the expression of many of the *Fgfr2*-regulated genes in Table 2 normalized their expression in the $Fgfr2/Pten^{\Delta/\Delta}$ lenses (Fig. 4b).

Despite the ability of *Pten* deletion to rescue lens cell survival in *Fgfr2*-deleted mice, our analysis revealed a number of genes related to apoptosis remain deregulated in $Fgfr2/Pten^{\Delta/\Delta}$ lenses. GO analysis revealed an enrichment in genes related to apoptotic processes, the cell cycle, and the p53 signaling pathway in both up- and downregulated genes from $Fgfr2/Pten^{\Delta/\Delta}$ lenses (Fig. 4c, Online Resource 5). In particular, some interesting upregulated genes include the cyclin dependent kinase inhibitor *Ccnd2*, *Cdkn1a* (aka $p21^{Cip1}$), *Gadd45 g* (a cellular stress response gene) (Vairapandi et al. 2002), *Serpine1* (a serine protease inhibitor) (Horowitz et al. 2008), and *Sesn2* (a p53 regulated stress protein) (Budanov et al. 2002). Given this observation, these genes may represent *Fgfr2* regulated transcripts that lack co-regulation by PTEN.

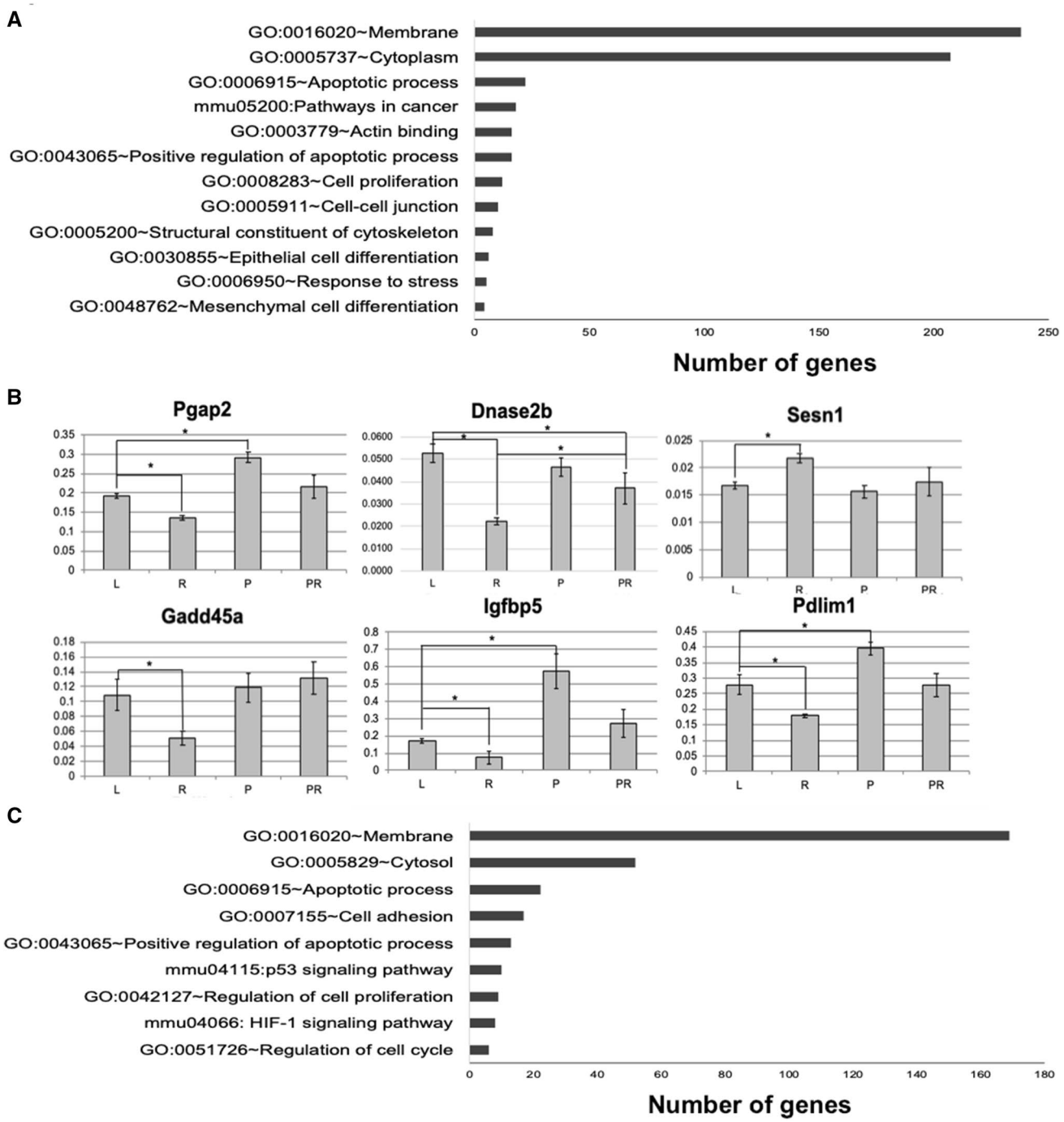

Fig. 4 **a** Top DAVID GO terms for downregulated DEGs in $Fgfr2^{\Delta/\Delta}$ lenses. **b** RT-qPCR validation of select downregulated DEGs in $Fgfr2^{\Delta/\Delta}$ lenses. *L* = *Le-Cre*; *R* = $Fgfr2^{\Delta/\Delta}$; *P* = $Pten^{\Delta/\Delta}$; *PR* = *Fgfr2/Pten*$^{\Delta/\Delta}$ lenses. Asterix (*) indicates $p < 0.05$. **c** Top DAVID GO terms for downregulated DEGs in *Fgfr2/Pten*$^{\Delta/\Delta}$ lenses

Analysis of lens fiber cell differentiation-related genes

In addition to widespread apoptosis, mouse lens fiber cells lacking *Fgfr2* in early development also fail to undergo normal fiber cell differentiation, which also contributes to the microphakia phenotype. In particular, $Fgfr2^{\Delta/\Delta}$ lens fiber cells fail to fully elongate or to properly exit the cell cycle (Chaffee et al. 2016). Therefore, we focused on how our dataset might explain defective fiber cell differentiation observed in these lenses. Genes related to cell–cell junction, cell proliferation, actin binding and the structural

constituent of the cytoskeleton all exhibited deregulation in *Fgfr2*$^{\Delta/\Delta}$ lenses (Fig. 4a). Of particular interest, a gene of the γ-crystallin family (*Crygc*) of fiber cell-specific proteins is downregulated in *Fgfr2*$^{\Delta/\Delta}$ lenses and restored to control (*Le-Cre*) levels in *Fgfr2/Pten*$^{\Delta/\Delta}$ lenses. In addition, *Fgfr2*$^{\Delta/\Delta}$ lenses exhibit reduced expression of *Dnase2b* (a gene essential for lens fiber cell denucleation) and *Pten* loss partially restores *Dnase2b* expression in *Fgfr2*-deficient lenses (Fig. 4b).

To provide insight of how *Fgfr2* deletion affects fiber cell differentiation, we used iSyTE (integrated Systems Tool for Eye gene discovery) (Kakrana et al. 2018) to compare the *Fgfr2*$^{\Delta/\Delta}$ DEGs (from RNA-seq data) with iSyTE developmental lens expression data from wild-type lenses at embryonic and newborn stages. Expression data from E16.5 lenses (Fig. 5a) captures the early stages of secondary lens fiber cell differentiation in mice (Cvekl and Ashery-Padan 2014). This analysis revealed that the majority of downregulated transcripts in newborn *Fgfr2*$^{\Delta/\Delta}$ lenses come from those genes specifically enriched in E16.5 lenses while the upregulated genes do not exhibit any such bias for lens enrichment at this stage. This analysis supports a specific role for *Fgfr2* in regulating genes required for lens fiber cell differentiation.

Since fiber cells differentiate from lens epithelial cells, the genes differentially regulated between these two cell types will reveal the genes important in distinguishing fiber cells from epithelial cells. To determine the relevance of FGFR2 signaling on fiber cell differentiation we compared our newborn *Fgfr2*$^{\Delta/\Delta}$ lens RNA-Seq data to isolated P0 lens fiber and epithelium expression data from Hoang et al. (2014) (Fig. 5b). *Fgfr2* deletion causes down-regulation of 319 genes from those highly enriched in wild-type lens fiber cells at P0, and upregulation of 455 genes that exhibit enriched expression in the lens epithelium. This transcriptomic change corresponds to a shift away from the differentiated lens fiber cell type towards the precursor lens epithelial cell type in the absence of *Fgfr2*.

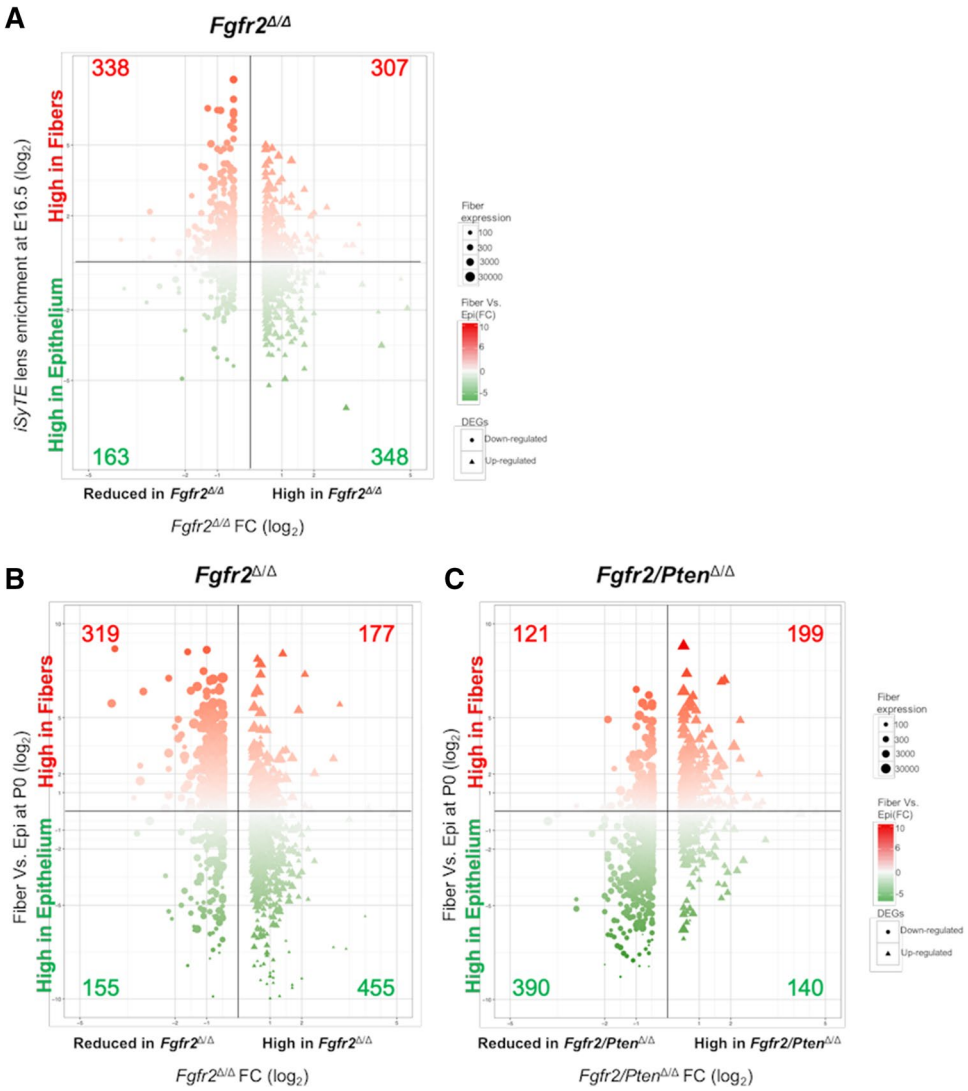

Fig. 5 **a** Volcano plot of iSyTE lens epithelium or fiber cell enriched genes at embryonic day E16.5 that are either reduced (downregulated) or high (upregulated) DEGs in *Fgfr2*$^{\Delta/\Delta}$ lenses. Numbers correspond to the number of genes in those parameters. (E, F) Volcano plots of iSyTE lens epithelium or fiber cell expressed genes at postnatal day 0 that are either reduced (downregulated) or high (upregulated) DEGs in *Fgfr2*$^{\Delta/\Delta}$ (**b**) or *Fgfr2/Pten*$^{\Delta/\Delta}$ (**c**) lenses. Numbers correspond to the number of genes in those parameters

Given that the loss of *Pten* normalizes 59.1% of the DEGs in the *Fgfr2*$^{\Delta/\Delta}$ lenses, we asked if the rescued DEGs represented a restoration of fiber cell gene expression. The *Fgfr2/Pten*$^{\Delta/\Delta}$ lenses exhibited downregulation of only 121 genes from the fiber-enriched category (compared to 319 in the *Fgfr2*$^{\Delta/\Delta}$ lenses) and upregulation of only 140 genes (compared to 455 in the *Fgfr2*$^{\Delta/\Delta}$ lenses) from the lens epithelium enriched category (Fig. 5c). The notable trend of this data demonstrates that 40.5% of downregulated genes in *Fgfr2*$^{\Delta/\Delta}$ lenses are fiber cell enriched, while only 17.9% of downregulated genes in *Fgfr2/Pten*$^{\Delta/\Delta}$ lenses are fiber cell enriched. This indicates that the additional loss of *Pten* restores the lost fiber cell identity in *Fgfr2*$^{\Delta/\Delta}$ lenses. Additionally, epithelial cell enriched genes make up 68.8% of upregulated genes in *Fgfr2*$^{\Delta/\Delta}$ lenses, while only 31% of upregulated genes in *Fgfr2/Pten*$^{\Delta/\Delta}$ lenses are epithelial cell enriched. While only 155 genes that are lens-epithelium enriched were downregulated in *Fgfr2*$^{\Delta/\Delta}$ lenses, in the *Fgfr2/Pten*$^{\Delta/\Delta}$ lenses, this number was increased to 390, indicating a loss of lens epithelium identity in the rescue animals. This suggests that *Pten* deletion restores fiber cell transcriptome in FGFR2 deficient lenses.

Molecular basis of microphakia rescue in *Fgfr2/Pten*$^{\Delta/\Delta}$ mice

Selecting the *Fgfr2*-regulated genes that play the most pivotal roles in the regulation of lens differentiation and survival represents a fundamental challenge. Since the rescue of microphakia occurs due to *Pten* deletion, the remainder of this manuscript focuses solely on genes directly regulated by a counterbalance of signals emanating from both FGFR2 and PTEN. We considered two sets of parameters to place those genes regulated by FGFR2 and PTEN, and at least partially rescued to control levels in *Fgfr2/Pten*$^{\Delta/\Delta}$ lenses into two categories. Category 1 comprises 28 genes which are downregulated in *Fgfr2*$^{\Delta/\Delta}$ relative to *Le-Cre*, upregulated in *Pten*$^{\Delta/\Delta}$ relative to *Le-Cre*, and upregulated or not changed in *Fgfr2/Pten*$^{\Delta/\Delta}$ relative to *Pten*$^{\Delta/\Delta}$. Category 2 consists of 40 genes downregulated genes in *Fgfr2*$^{\Delta/\Delta}$ relative to *Le-Cre*, upregulated in *Pten*$^{\Delta/\Delta}$ relative to *Le-Cre*, and upregulated or not changed in *Fgfr2/Pten*$^{\Delta/\Delta}$ relative to *Fgfr2*$^{\Delta/\Delta}$ (Fig. 6a, Table 5). RT-qPCR validated the differential expression of many of these total 68 genes in all four genotypes (Online Resource 7).

While the genes in categories 1 and 2 encode a number of different kinds of proteins, we focused on transcription factors given the importance of transcriptional regulation for differentiation and morphogenesis. Zinc-finger, and regulation of transcription were among the GO analysis terms enriched in the 68 genes from categories 1 and 2 (Fig. 6b). In particular, transcription factors *Nkx6-1*, *Evx2*, and *Gata6* from category 2 play important roles in morphogenesis, but have no recognized role in lens development. *Nkx6-1* antagonizes the activity of *Pax6* in both ventral neural patterning and in endocrine pancreatic cell specification (McMahon 2000; Qiu et al. 1998; Sander et al. 2000; Schaffer et al. 2010, 2013; Henseleit et al. 2005; Taylor et al. 2013). *Evx2* has homology to *Drosophila melanogaster* even-skipped (D'Esposito et al. 1991), a pair-rule gene important in embryo segmentation. *Gata6,* a zinc-finger transcription factor, participates in the development of many tissues, including the heart and pancreas (Morrisey et al. 1996). Given the central importance of transcription factors as master regulators of tissue identity and function, we hypothesized that *Nkx6-1*, *Evx2*, and/or *Gata6* may function as key regulators of FGFR signaling in morphogenesis.

To explore the potential role of *Nkx6-1*, *Evx2*, and *Gata6* in the lens and prioritize them for further study, we first determined the relative expression level of these genes in the developing lens using iSyTE. According to iSyTE, *Nkx6-1* expression and enrichment in the lens peaks at E16.5. In contrast, although *Evx2* expression is enriched in lens, its expression level remains moderate and unchanged throughout lens development. *Gata6* exhibits the lowest lens expression with no lens enrichment throughout development (Fig. 7a). RT-qPCR revealed that *Nkx6-1* and *Gata6* expression declined in *Fgfr2*$^{\Delta/\Delta}$ lenses, but the expression of both of these genes normalized to the *Le-Cre* level in the *Fgfr2/Pten*$^{\Delta/\Delta}$ lenses. Although the expression of *Evx2* declined in the *Fgfr2*$^{\Delta/\Delta}$ lenses, the transcript level of this gene remained insignificantly different among all genotypes (Fig. 7b). The high expression of *Nkx6-1* during the onset of secondary fiber cell differentiation, its enrichment in the normal lens, and its regulation by both FGFR2 and PTEN, led us to focus our investigations on *Nkx6-1* as providing an alternative shunt to mediate downstream targets of FGFR signaling in the absence of FGFR2.

Because sequence-specific DNA-binding is key to transcription factor function, we sought to identify the DNA-binding motifs for NKX6-1 and to determine if category 1 and/or category 2 genes contain this binding motif in their regulatory regions. An examination of the DNA-binding motifs for NKX6-1 using MotifDB software (Fig. 8a) revealed the consensus sequence for NKX6-1. To search for NKX6-1 binding sites, we scanned the putative promoter region (defined as 2500 bp upstream of the transcription start site) of category 1 and category 2 genes for relevant binding motifs. In total, the putative promoter regions of 53 of the 68 genes contained at least one binding motif for NKX6-1, placing *Nkx6-1* at the center of a regulatory network of these genes (Online Resource 8). Based on this information, we hypothesized that *Pten* deletion-induced rescue of survival and fiber cell differentiation in *Fgfr2*-deleted lenses depends on NKX6-1 regulatory control of target genes.

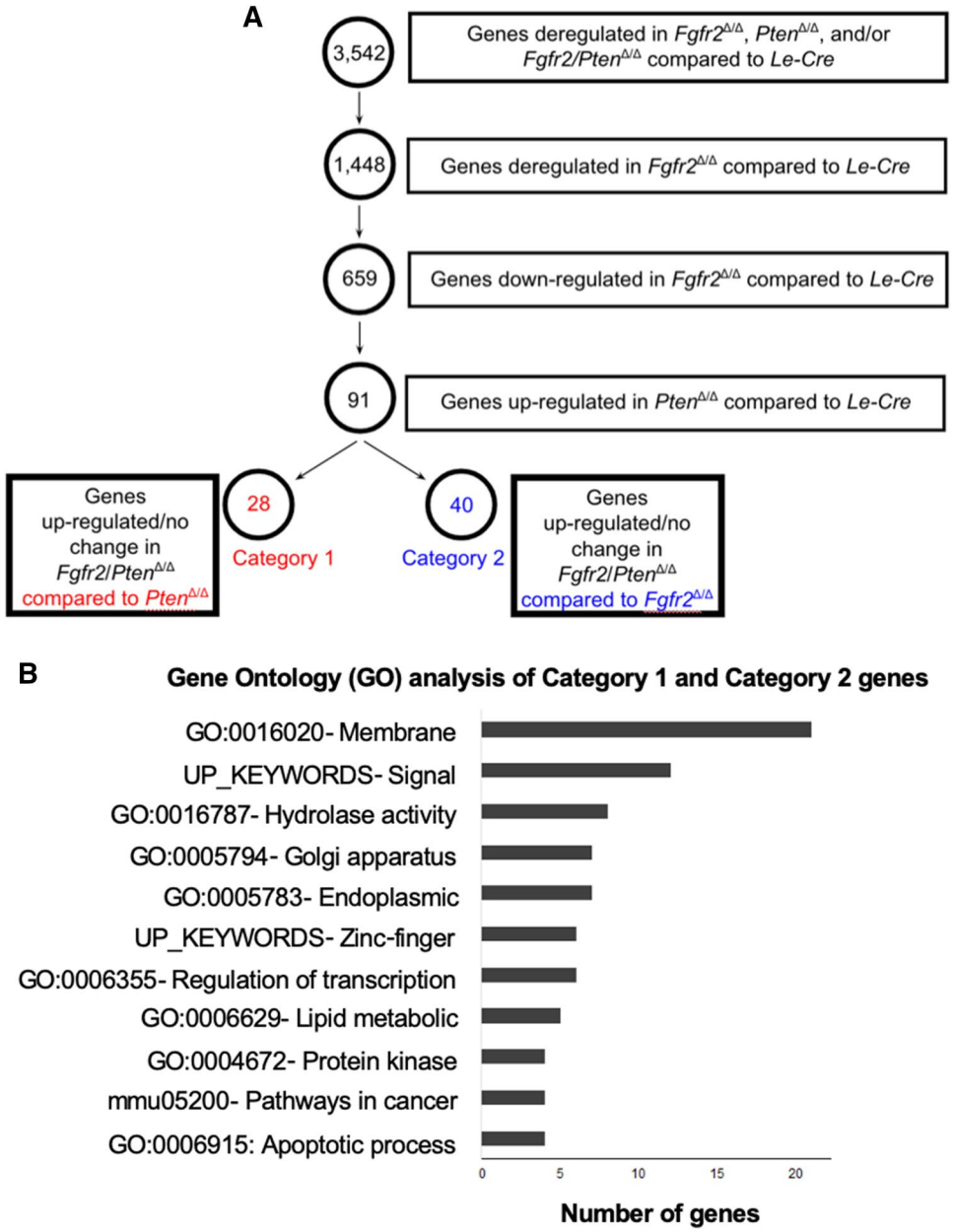

Fig. 6 **a** Parameters (boxed) and number of genes fitting those parameters (circled) set to define categories 1 and 2 of candidate genes. **b** Top DAVID GO terms for 68 category 1 and 2 genes

Table 5 List of candidate genes from category 1 and category 2

Category 1	Category 2
Ada1, *Birc7*, *Cdr2*, *Chst7*, *Doc2b*, *Dock8*, *Fabp5*, *Gm13091*, *Gm14418*, *Gm 20631*, *Gm2895*, *Hmgn3*, *Ifit2*, *Nap1l2*, *Ogn*, *Olfml3*, *Podn*, *Ppm1e*, *Ppp1r3c*, *Saraf*, *Snapc1*, *Tmem68*, *Tmprss11e*, *Ttc39b*, *Wdr33*, *1700019D03Rik*, *1700086L19Rik*, *4930502E18Rik*	*Acer2*, *Alox15*, *Avp*, *B930036N10Rik*, *Ccdc117*, *Ccser1*, *Ces5a*, *Chrm3*, *Colec11*, *Csmd2*, *Csrp1*, *Dbpht2*, *Dgat2*, *Evx2*, *Fgfr2*, *Frmd6*, *Gata6*, *Gm14170*, *Gm37142*, *Igfbp5*, *Insm1*, *Kifc3*, *Klhl32*, *Lctl*, *Lipg*, *Mt1*, *Nat6*, *Nkx6-1*, *Pcsk2*, *Ppp2r5e*, *Prokr1*, *Prox1os*, *Ptk6*, *Rasgrp1*, *Ripk4*, *Rnf180*, *Slc2a9*, *Tigd2*, *2810468N07Rik*, *9430020K01Rik*

Given the major signal transduction cascades initiated by FGFR signaling in cells, we examined the category 1 and 2 genes with NKX6-1 binding motifs as potential mediators of intracellular signaling. One gene *Rasgrp1* (Ras guanyl-releasing protein 1) stood out as it is a known activator of both the PI3 K-AKT (Ong et al. 2001) and the Ras/Raf/MEK/ERK signaling cascade (Ebinu et al. 1998). RT-qPCR validated the differential expression of *Rasgrp1* in all genotypes (Online Resource 7). The obvious connection of *Rasgrp1* to ERK1/2 activation, a known mediator of FGFR

A

Expression	E10.5	E11.5	E12.5	E16.5	E17.5	E19.5	P0	P2	P28	P56
Nkx6-1	41.20	31.94	30.19	94.02	55.86	45.34	57.73	61.38	44.06	60.36
Gata6	13.98	19.79	20.86	27.44	24.59	25.97	26.08	24.35	24.88	19.25
Evx2	33.48	43.8	54.11	53.35	48.69	50.28	60.6	57.84	47.2	43.39
Enrichment	**E10.5**	**E11.5**	**E12.5**	**E16.5**	**E17.5**	**E19.5**	**P0**	**P2**	**P28**	**P56**
Nkx6-1	-1.99	-1.92	-2.07	1.26	-1.30	-1.64	-1.27	-1.24	-1.75	-1.30
Gata6	-4.18	-3.30	-2.63	-2.11	-2.52	-2.30	-2.27	-2.27	-2.69	-3.08
Evx2	-1.17	-1.05	1.18	1.17	1.12	1.12	1.33	1.19	-1.03	1.05

B

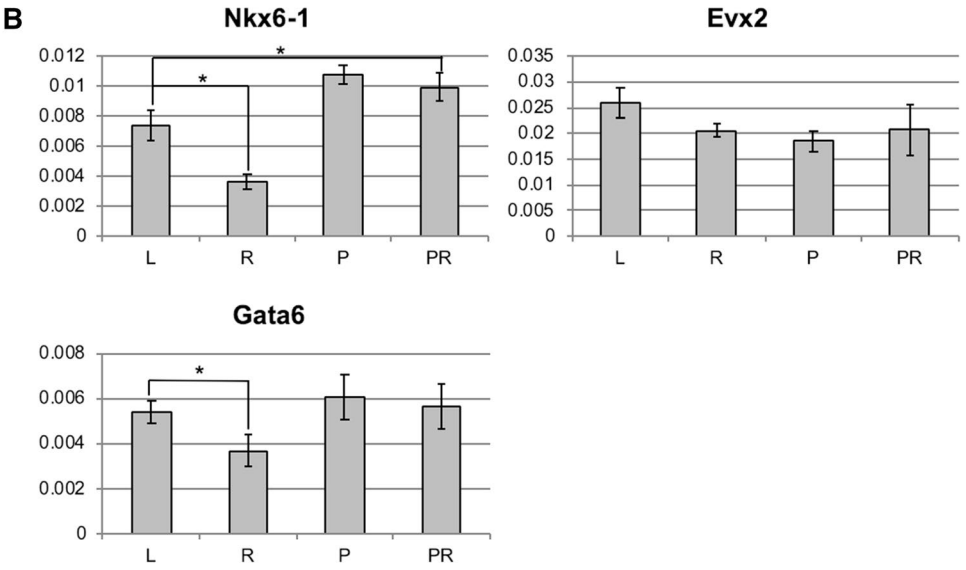

Fig. 7 **a** iSyTE lens expression and enrichment data for *Nkx6-1, Evx2,* and -*Gata6* through embryonic and postnatal development. Red indicates high expression or enrichment, white indicates moderate expression or enrichment, and green indicates low expression or enrichment. **b** RT-qPCR validation of *Nkx6-1, Evx2,* and *Gata6* expression in lenses of all four genotypes. $L = Le\text{-}Cre$; $R = Fgfr2^{\Delta/\Delta}$; $P = Pten^{\Delta/\Delta}$; $PR = Fgfr2/Pten^{\Delta/\Delta}$. Asterix (*) indicates $p < 0.05$

A

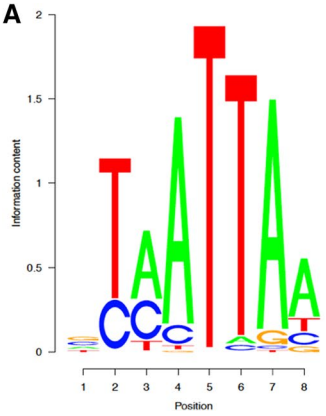

B

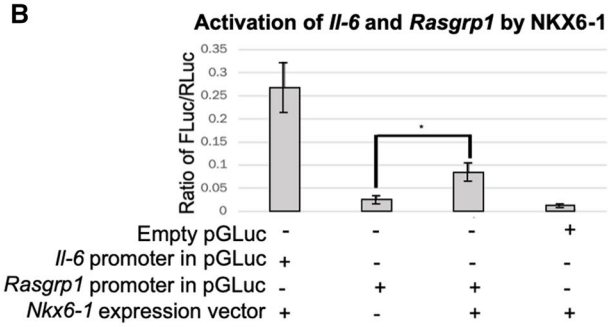

Fig. 8 **a** Transcription factor binding motif for NKX6-1. **b** Activation of *Il-6* and *Rasgrp1* by NKX6-1. pGLuc is the luciferase vector; The Il-6 promoter constitutes a 2500 bp region upstream of the *Il-6* transcriptional start site (TSS) cloned into pGLuc. The *Rasgrp1* promoter constitutes a 2500 bp region upstream of the *Rasgrp1* TSS cloned into pGLuc. The *Nkx6-1* expression vector provided for NKX6-1 expression as indicated

signaling, identified this gene as an important potential node to explain how the deletion of *Pten* orchestrates the rescue of the FGFR2-deficient lens transcriptome.

To test the hypothesis that NKX6-1 regulates key proteins involved in the rescue of lens development in $Fgfr2/Pten^{\Delta/\Delta}$ lenses, we designed a luciferase assay in which we measured the ability of NKX6-1 to activate *Rasgrp1* expression in the lens epithelial cell line, 21EM15 (Reddan et al. 1989). The *Il-6* promoter, a known target of NKX6-1 (Li et al. 2016), provided a positive control for transcriptional activation by NKX6-1, while a promoter-less luciferase vector provided a negative control. Overexpression of *Nkx6-1* significantly increased the amount of firefly luciferase driven by the *Rasgrp1* promoter, indicating that NKX6-1 can upregulate *Rasgrp1* expression in vivo (Fig. 8b). This establishes a new regulatory relationship between NKX6-1 and *Rasgrp1* by uncovering a novel regulatory module between transcription and signaling.

Discussion

Tissue morphogenesis relies on the coordination of transcriptional networks downstream of many simultaneous signaling pathways. FGF/FGFR-signaling regulates the development of many tissues in both invertebrates and vertebrates, but how FGFR signaling is regulated during morphogenesis, and how alterations in these events results in developmental defects, remains incomplete. Many extracellular signals, including FGFs, converge on key intracellular mediators, such as ERK and AKT to drive changes in cellular fate. The activation level of ERK1/2 and AKT appear to function as cellular rheostats that control cell proliferation, survival and differentiation. Signaling mechanisms such as these provide an example of switch-like behavior that result in developmental robustness by providing alternative mechanisms to achieve similar downstream outcomes (Ferrell 1996). Several recent examples demonstrate the regulation of FGFR signaling in vertebrates by PTEN (Chaffee et al. 2016; Guntur et al. 2011; Scioli et al. 2014; Hertzler-Schaefer et al. 2014). To explore this regulatory relationship further, we exploited the simplicity of the developing lens to identify alternative molecular mechanisms regulated by PTEN that can compensate for the loss of FGFR2 signaling during development.

We discovered that while *Fgfr2* deletion in lenses causes dramatic deregulation of global gene expression compared to control (*Le-Cre*) lenses, simultaneous *Pten* deletion shifts the transcriptome back towards that of *Le-Cre*. These RNA-seq based transcriptomic studies provide insights into the molecular basis of both the microphakia in $Fgfr2^{\Delta/\Delta}$ lenses and the rescue of lens size and development provided by simultaneous *Pten* deletion. FGFR2 loss in the lens most dramatically affects cell survival and differentiation, so we focused our analysis on these two aspects of lens development. Gene ontology analysis and iSyTE expression data revealed pathways that may explain the widespread apoptosis in $Fgfr2^{\Delta/\Delta}$ lenses, and the rescue of survival caused by *Pten* deletion. Genes related to the p53 signaling pathway, caspase activity, and BAX-mediated apoptosis are deregulated in $Fgfr2^{\Delta/\Delta}$ lenses, but many of the genes associated with these pathways exhibit normalized expression in $Fgfr2/Pten^{\Delta/\Delta}$ lenses. The restoration of expression of these p53-related genes likely explains the low levels of apoptosis in $Fgfr2/Pten^{\Delta/\Delta}$ lenses relative to the $Fgfr2^{\Delta/\Delta}$ lenses.

Our transcriptomic data build a strong case for the instructive role of FGFR signaling in fiber cell differentiation. The best visualization of this point comes from Fig. 5 where the transcriptomes of the $Fgfr2^{\Delta/\Delta}$ and $Fgfr2/Pten^{\Delta/\Delta}$ lenses are compared to wild-type gene expression data compiled by iSyTE. This comparison shows that the $Fgfr2^{\Delta/\Delta}$ lens transcriptome shifts to a more lens epithelial character in comparison to the transcriptomes of wild-type lenses at both the onset of secondary fiber cell differentiation (E16.5) and at P0. Specific examples include *Crygc* (encoding an important lens fiber cell structural protein) which exhibits reduced expression in $Fgfr2^{\Delta/\Delta}$ lenses, but normalized expression in $Fgfr2/Pten^{\Delta/\Delta}$ lenses, and *Dnase2b* (essential for fiber cell denucleation) with significantly reduced expression in $Fgfr2^{\Delta/\Delta}$ lenses, and a partial restoration of expression in $Fgfr2/Pten^{\Delta/\Delta}$ lenses. Together, our data indicate that fiber cells lose their identity in $Fgfr2^{\Delta/\Delta}$ lenses, but regain many aspects of fiber cell identity with simultaneous *Pten* deletion. The restoration of fiber cell elongation by *Pten* deletion likely plays a significant role in the rescue of microphakia in FGFR2-deficient lenses.

The genes directly regulated by both FGFR2 and PTEN that have the greatest potential to impact the activation of ERK1/2 or AKT provide the best candidates to explain the restoration of developmental homeostasis in lenses lacking both *Fgfr2* and *Pten*. Among the genes identified in categories 1 and 2, we identified *Rasgrp1* as a candidate gene having the potential to increase the activation of both ERK1/2 and AKT. RASGRP1 acts as a guanyl exchange factor to activate RAS. Activated RAS, in turn, activates RAF, upstream of ERK1/2 activation, and p110, the catalytic subunit of PI3 K, upstream of AKT activation. Having identified *Rasgrp1* as a high-priority candidate, we searched among the other candidates to provide a mechanism to increase the level of RASGRP1 in the $Fgfr2/Pten^{\Delta/\Delta}$ lenses.

Among the transcription factors identified in the categories of genes regulated by both FGFR2 and PTEN, NKX6-1 provides a strong candidate to drive the upregulation of *Rasgrp1* expression. *Rasgrp1* and most of the genes in categories 1 and 2 contain the binding motif for NKX6-1 within their putative promoter regions. Our luciferase assay suggests that NKX6-1 upregulates the expression of *Rasgrp1* in vivo. These findings point to NKX6-1 as a transcription factor with a previously unappreciated role in regulating survival and fiber cell differentiation in $Fgfr2/Pten^{\Delta/\Delta}$ lenses as well as provide an important output of FGFR-regulated transcription in the development of other tissues.

Although NKX6-1 antagonizes PAX6 during patterning of the neural tube and pancreas (Taylor et al. 2013), and *Pax6* mutations cause human microphthalmia (Verma and Fitzpatrick 2007), the role of NKX6-1 in lens development is undefined. According to iSyTE, *Pax6* expression is high in the lens epithelium but falls as epithelial cells differentiate into lens fibers. In contrast, while *Nkx6-1* is expressed in the lens as early as E10.5, its expression and enrichment peaks precisely when secondary fiber cell differentiation initiates. Given the association of FGFR-signaling and fiber cell

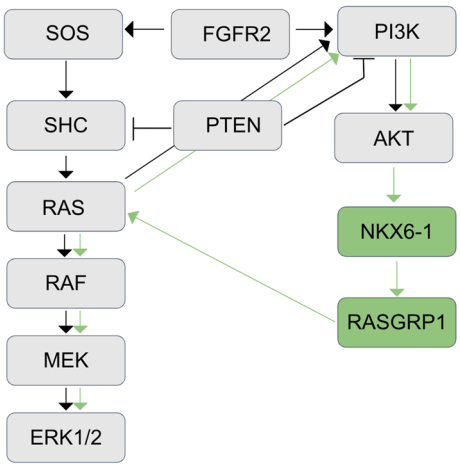

Fig. 9 Identification of a novel regulatory shunt to rescue ERK and AKT activation in the absence of *Fgfr2* and *Pten*. PTEN antagonizes the activation of ERK1/2 by dephosphorylating SHC and AKT by reversing the reaction catalyzed by PI3 K. In the absence of PTEN, NKX6-1 levels are restored, leading to direct upregulation of *Rasgrp1* expression. RASGRP1 can then activate RAS, which offers an alternate shunt to activate the FGFR2 downstream effectors, RAF and PI3 K to restore ERK and AKT activation, respectively. Novel relationships identified in this work are highlighted in green

differentiation, antagonism of PAX6 transcriptional activity by FGF-induced NKX6-1 expression presents an interesting novel mechanism to regulate lens development. Alternatively, it remains possible that NKX6-1 provides a specific mechanism to rescue transcription during both primary and secondary fiber cell differentiation in *Fgfr2/Pten*$^{\Delta/\Delta}$ lenses while only playing a minor role in normal lens development. Future mechanistic studies concerning the requirement for *Nkx6-1* in lens development will distinguish between these possibilities.

Here, we have demonstrated that FGFR2-signaling can regulate the transcription of genes required for cell differentiation and survival. However, in the absence of FGFR2, the deletion of *Pten* opens alternative pathways to restore the transcriptional regulation of many genes important for *Fgfr2* downstream effectors that control these processes. Specifically, simultaneous deletion of *Pten* results in increased AKT activation which in turn upregulates the expression of *Nkx6-1* (Zhang et al. 2014). NKX6-1 upregulates *Rasgrp1* expression, to activate an alternate "shunt" pathway involving both AKT and ERK1/2 phosphorylation. Thus, in the absence of PTEN, signals downstream of FGFR2 can still occur, rescuing microphakia despite the loss of *Fgfr2*. We present a model to define this new connection between FGFR signaling, the homeodomain transcription factor NKX6-1, and its downstream PI3 K and MAPK cascade regulator RASGRP1 (Fig. 9). Furthermore, these data offer new areas of investigation to explore the generality of this regulatory module in numerous other developmental disorders involving FGFR2 and PTEN pathways, including craniosynostosis and cancer.

Acknowledgements 21EM15 cells were generously provided by Dr. John R. Reddan (Professor Emeritus, Department of Biological Sciences, Oakland University, Rochester, MI). RNA sequencing was completed at the Sequencing Core Laboratory at the University of Cincinnati. The raw and processes data files are deposited to NCBI GEO (accession number GSE132945). We acknowledge and thank the staff (Dr. Andor Kiss & Ms. Xiaoyun Deng) of the Center for Bioinformatics and Functional Genomics (CBFG) at Miami University for instrumentation and computational support.

Funding This work was supported by an National Institute of Health (NIH) grant R01 EY012995 awarded to M.L.R. S.A.L. was supported by NIH grant R01 EY021505.

Compliance with ethical standards

Conflict of interest The authors declare that they have no conflict of interest.

Ethical approval All procedures were approved by the Miami University Institutional Animal Care and Use Committee and complied with the ARVO Statement for the Use of Animals in Research and consistent with those published by the Institute for Laboratory Animal Research (Guide for the Care and Use of Laboratory Animals).

References

Babina IS, Turner NC (2017) Advances and challenges in targeting FGFR signalling in cancer. Nat Rev Cancer 17(5):318–332

Bolger AM, Lohse M, Usadel B (2014) Trimmomatic: a flexible trimmer for Illumina sequence data. Bioinformatics 30(15):2114–2120

Budanov AV, Shoshani T, Faerman A, Zelin E, Kamer I, Kalinski H, Feinstein E et al (2002) Identification of a novel stress-responsive gene Hi95 involved in regulation of cell viability. Oncogene 21(39):6017–6031

Butler MG, Dasouki MJ, Zhou X-P, Talebizadeh Z, Brown M, Takahashi TN, Eng C et al (2005) Subset of individuals with autism spectrum disorders and extreme macrocephaly associated with germline PTEN tumour suppressor gene mutations. J Med Genet 42(4):318–321

Cavalheiro GR, Matos-Rodrigues GE, Zhao Y, Gomes AL, Anand D, Predes D, Martins RAP et al (2017) N-myc regulates growth and fiber cell differentiation in lens development. Dev Biol 429(1):105–117

Chaffee BR, Hoang TV, Leonard MR, Bruney DG, Wagner BD, Dowd JR, Robinson ML et al (2016) FGFR and PTEN signaling interact during lens development to regulate cell survival. Dev Biol 410(2):150–163

Chow RL, Roux GD, Roghani M, Palmer MA, Rifkin DB, Moscatelli DA, Lang RA (1995) FGF suppresses apoptosis and induces differentiation of fibre cells in the mouse lens. Development 121(12):4383–4393

Collins TN, Mao Y, Li H, Bouaziz M, Hong A, Feng G-S, Zhang X et al (2018) Crk proteins transduce FGF signaling to promote lens fiber cell elongation. Life. https://doi.org/10.7554/eLife.32586

Cvekl A, Ashery-Padan R (2014) The cellular and molecular mechanisms of vertebrate lens development. Development 141(23):4432–4447

Cvekl A, Zhang X (2017) Signaling and Gene regulatory networks in mammalian lens development. Trends Genet TIG 33(10):677–702
D'Esposito M, Morelli F, Acampora D, Migliaccio E, Simeone A, Boncinelli E (1991) EVX2, a human homeobox gene homologous to the even-skipped segmentation gene, is localized at the 5′ end of HOX4 locus on chromosome 2. Genomics 10(1):43–50
De Maria A, Bassnett S (2015) Birc7: a late fiber gene of the crystalline lens. Invest Ophthalmol Vis Sci 56(8):4823–4834
Ebinu JO, Bottorff DA, Chan EY, Stang SL, Dunn RJ, Stone JC (1998) RasGRP, a Ras guanyl nucleotide- releasing protein with calcium- and diacylglycerol-binding motifs. Science 280(5366):1082–1086
Ferrell JE Jr (1996) Tripping the switch fantastic: how a protein kinase cascade can convert graded inputs into switch-like outputs. Trends Biochem Sci 21(12):460–466
Garcia CM, Yu K, Zhao H, Ashery-Padan R, Ornitz DM, Robinson ML, Beebe DC (2005) Signaling through FGF receptor-2 is required for lens cell survival and for withdrawal from the cell cycle during lens fiber cell differentiation. Dev Dyn Off Publ Am Assoc Anat 233(2):516–527
Garcia CM, Huang J, Madakashira BP, Liu Y, Rajagopal R, Dattilo L, Beebe DC et al (2011) The function of FGF signaling in the lens placode. Dev Biol 351:176–185. https://doi.org/10.1016/j.ydbio.2011.01.001
Gu J, Tamura M, Yamada KM (1998) Tumor suppressor PTEN inhibits integrin- and growth factor–mediated mitogen-activated protein (MAP) kinase signaling pathways. J Cell Biol 143:1375–1383. https://doi.org/10.1083/jcb.143.5.1375
Guntur AR, Reinhold MI, Cuellar J Jr, Naski MC (2011) Conditional ablation of Pten in osteoprogenitors stimulates FGF signaling. Development 138(7):1433–1444
Henseleit KD, Nelson SB, Kuhlbrodt K, Hennings JC, Ericson J, Sander M (2005) NKX6 transcription factor activity is required for alpha- and beta-cell development in the pancreas. Development 132(13):3139–3149
Hertzler-Schaefer K, Mathew G, Somani A-K, Tholpady S, Kadakia MP, Chen Y, Zhang X et al (2014) Pten loss induces autocrine FGF signaling to promote skin tumorigenesis. Cell Rep 6(5):818–826
Hoang TV, Kumar PKR, Sutharzan S, Tsonis PA, Liang C, Robinson ML (2014) Comparative transcriptome analysis of epithelial and fiber cells in newborn mouse lenses with RNA sequencing. Mol Vis 20:1491–1517
Hollander MC, Blumenthal GM, Dennis PA (2011) PTEN loss in the continuum of common cancers, rare syndromes and mouse models. Nat Rev Cancer 11(4):289–301
Horowitz JC, Rogers DS, Simon RH, Sisson TH, Thannickal VJ (2008) Plasminogen activation induced pericellular fibronectin proteolysis promotes fibroblast apoptosis. Am J Respir Cell Mol Biol 38(1):78–87
Huang DW, Sherman BT, Lempicki RA (2009) Systematic and integrative analysis of large gene lists using DAVID bioinformatics resources. Nat Protoc 4(1):44–57
Jin S, Mazzacurati L, Zhu X, Tong T, Song Y, Shujuan S, Zhan Q et al (2003) Gadd45a contributes to p53 stabilization in response to DNA damage. Oncogene 22(52):8536–8540
Kakrana A, Yang A, Anand D, Djordjevic D, Ramachandruni D, Singh A, Lachke SA et al (2018) iSyTE 2.0: a database for expression-based gene discovery in the eye. Nucleic Acids Res 46(D1):D875–D885
Kanai M, Göke M, Tsunekawa S, Podolsky DK et al (1997) Signal transduction pathway of human fibroblast growth factor receptor 3. J Biol Chem 272:6621–6628. https://doi.org/10.1074/jbc.272.10.6621
Klint P, Kanda S, Kloog Y, Claesson-Welsh L (1999) Contribution of Src and Ras pathways in FGF-2 induced endothelial cell differentiation. Oncogene 18(22):3354–3364
Knobloch J, Schmitz I, Götz K, Schulze-Osthoff K, Rüther U (2008) Thalidomide induces limb anomalies by PTEN stabilization, Akt suppression, and stimulation of caspase-dependent cell death. Mol Cell Biol 28(2):529–538
Lam PT, Padula SL, Hoang TV, Poth JE, Liu L, Liang C, Robinson ML et al (2019) Considerations for the use of Cre recombinase for conditional gene deletion in the mouse lens. Human Genomics 13(1):10
Li H, Tao C, Cai Z, Hertzler-Schaefer K, Collins TN, Wang F, Zhang X et al (2014) Frs2 and Shp2 signal independently of Gab to mediate FGF signaling in lens development. J Cell Sci 127:571–582. https://doi.org/10.1242/jcs.134478
Li W, Itou J, Tanaka S, Nishimura T, Sato F, Toi M (2016) A homeobox protein, NKX6.1, up-regulates interleukin-6 expression for cell growth in basal-like breast cancer cells. Exp Cell Res 343(2):177–189
Li H, Mao Y, Bouaziz M, Yu H, Qu X, Wang F, Zhang X et al (2019) Lens differentiation is controlled by the balance between PDGF and FGF signaling. PLoS Biol 17(2):e3000133
Liaw D, Marsh DJ, Li J, Dahia PL, Wang SI, Zheng Z, Parsons R et al (1997) Germline mutations of the PTEN gene in Cowden disease, an inherited breast and thyroid cancer syndrome. Nat Genet 16(1):64–67
Lovicu FJ, Overbeek PA (1998) Overlapping effects of different members of the FGF family on lens fiber differentiation in transgenic mice. Development 125(17):3365–3377
Madakashira BP, Kobrinski DA, Hancher AD, Arneman EC, Wagner BD, Wang F, Robinson ML et al (2012) Frs2 enhances fibroblast growth factor-mediated survival and differentiation in lens development. Development 139:4601–4612. https://doi.org/10.1242/dev.081737
Marie PJ, Coffin JD, Hurley MM (2005) FGF and FGFR signaling in chodrodysplasias and craniosynostosis. J Cell Biochem 96(5):888–896. https://doi.org/10.1002/jcb.20582
Masumoto J, Taniguchi S, Sagara J (2001) Pyrin N-terminal homology domain- and caspase recruitment domain-dependent oligomerization of ASC. Biochem Biophys Res Commun 280(3):652–655
McAvoy JW, Chamberlain CG (1989) Fibroblast growth factors (FGF) induces different responses in lens epithelial cells depending on its concentration. Cell Diff Devel. https://doi.org/10.1016/0922-3371(89)90129-9
McIntosh I, Bellus GA, Jab EW (2000) The pleiotropic effects of fibroblast growth factor receptors in mammalian development. Cell Struct Funct 25(2):85–96
McMahon AP (2000) Neural patterning: the role of Nkx genes in the ventral spinal cord. Genes Dev 14:2261–2264
Mohammadi M, Dikic I, Sorokin A, Burgess WH, Jaye M, Schlessinger J (1996) Identification of six novel autophosphorylation sites on fibroblast growth factor receptor 1 and elucidation of their importance in receptor activation and signal transduction. Mol Cell Biol 16(3):977–989
Morrisey EE, Ip HS, Lu MM, Parmacek MS (1996) GATA-6: a zinc finger transcription factor that is expressed in multiple cell lineages derived from lateral mesoderm. Dev Biol 177(1):309–322
Myers MP, Stolarov JP, Eng C, Li J, Wang SI, Wigler MH, Tonks NK et al (1997) P-TEN, the tumor suppressor from human chromosome 10q23, is a dual-specificity phosphatase. Proc Natl Acad Sci 94:9052–9057. https://doi.org/10.1073/pnas.94.17.9052
Ong SH, Hadari YR, Gotoh N, Guy GR, Schlessinger J, Lax I (2001) Stimulation of phosphatidylinositol 3-kinase by fibroblast growth factor receptors is mediated by coordinated recruitment of multiple docking proteins. Proc Natl Acad Sci USA 98(11):6074–6079
Pilarski R (2019) Hamartoma tumor syndrome: a clinical overview. Cancers. https://doi.org/10.3390/cancers11060844
Qiu M, Shimamura K, Sussel L, Chen S, Rubenstein JL (1998) Control of anteroposterior and dorsoventral domains of Nkx-6.1 gene

expression relative to other Nkx genes during vertebrate CNS development. Mech Dev 72:77–88
Reddan JR, Kuck JF, Dziedzic DC, Kuck KD, Reddan PR, Wasielewski P (1989) Establishment of lens epithelial cell lines from Emory and cataract resistant mice and their response to hydrogen peroxide. Lens Eye Toxic Res 6(4):687–701
Robinson ML, Overbeek PA, Verran DJ, Grizzle WE, Stockard CR, Friesel R, Thompson JA et al (1995) Extracellular FGF-1 acts as a lens differentiation factor in transgenic mice. Development 121(2):505–514
Robinson MD, McCarthy DJ, Smyth GK (2010) edgeR: a Bioconductor package for differential expression analysis of digital gene expression data. Bioinformatics 26(1):139–140
Sander M, Paydar S, Ericson J, Briscoe J, Berber E, German M, Rubenstein JL et al (2000) Ventral neural patterning by Nkx homeobox genes: Nkx6.1 controls somatic motor neuron and ventral interneuron fates. Genes Dev 14(17):2134–2139
Sawh-Martinez R, Steinbacher DM (2019) Syndromic craniosynostosis. Clin Plast Surg 46(2):141–155
Schaffer AE, Freude KK, Nelson SB, Sander M (2010) Nkx6 transcription factors and Ptf1a function as antagonistic lineage determinants in multipotent pancreatic progenitors. Dev Cell 18:1022–1029
Schaffer AE, Taylor BL, Benthuysen JR, Liu J, Thorel F, Yuan W, Sander M et al (2013) Nkx6.1 controls a gene regulatory network required for establishing and maintaining pancreatic Beta cell identity. PLoS Genet 9(1):e1003274
Scioli MG, Bielli A, Gentile P, Mazzaglia D, Cervelli V, Orlandi A (2014) The biomolecular basis of adipogenic differentiation of adipose-derived stem cells. Int J Mol Sci 15(4):6517–6526
Sellitto C, Li L, Gao J, Robinson ML, Lin RZ, Mathias RT, White TW (2013) AKT activation promotes PTEN hamartoma tumor syndrome-associated cataract development. J Clin Investig 123(12):5401–5409
Stambolic V, Suzuki A, de la Pompa JL, Brothers GM, Mirtsos C, Sasaki T, Mak TW et al (1998) Negative regulation of PKB/Akt-dependent cell survival by the tumor suppressor PTEN. Cell 95(1):29–39
Tashima Y, Taguchi R, Murata C, Ashida H, Kinoshita T, Maeda Y (2006) PGAP2 is essential for correct processing and stable expression of GPI-anchored proteins. Mol Biol Cell 17(3):1410–1420
Taylor BL, Liu F-F, Sander M (2013) Nkx6.1 is essential for maintaining the functional state of pancreatic beta cells. Cell Rep 4:1262–1275
Trapnell C, Pachter L, Salzberg SL (2009) TopHat: discovering splice junctions with RNA-Seq. Bioinformatics 25(9):1105–1111
Trapnell C, Roberts A, Goff L, Pertea G, Kim D, Kelley DR, Pachter L et al (2012) Differential gene and transcript expression analysis of RNA-seq experiments with TopHat and Cufflinks. Nat Protoc 7(3):562–578
Trougakos IP, Lourda M, Antonelou MH, Kletsas D, Gorgoulis VG, Papassideri IS, Gonos ES et al (2009) Intracellular clusterin inhibits mitochondrial apoptosis by suppressing p53-activating stress signals and stabilizing the cytosolic Ku70-Bax protein complex. Clin Cancer Res 15(1):48–59
Vairapandi M, Balliet AG, Hoffman B, Liebermann DA (2002) GADD45b and GADD45 g are cdc2/cyclinB1 kinase inhibitors with a role in S and G2/M cell cycle checkpoints induced by genotoxic stress. J Cell Physiol 192(3):327–338
Verma AS, Fitzpatrick DR (2007) Anophthalmia and microphthalmia. Orphanet J Rare Dis 2:47
Wormstone I Michael, Wride Michael A (2011) The Ocular lens: a classic model for development, physiology and disease. Philos Trans R Soc Lond Ser B Biol Sci 366(1568):1190–1192 **(Print)**
Zhang T, Chen C, Breslin MB, Song K, Lan MS (2014) Extra-nuclear activity of INSM1 transcription factor enhances insulin receptor signaling pathway and Nkx6.1 expression through RACK1 interaction. Cell Signal 26(4):740–747
Zhao H, Yang T, Madakashira BP, Thiels CA, Bechtle CA, Garcia CM, Robinson ML et al (2008) Fibroblast growth factor receptor signaling is essential for lens fiber cell differentiation. Dev Biol 318:276–288. https://doi.org/10.1016/j.ydbio.2008.03.028

Publisher's Note Springer Nature remains neutral with regard to jurisdictional claims in published maps and institutional affiliations.